

LETTERS

A dynamic, rotating ring current around Saturn

S. M. Krimigis^{1,2}, N. Sergis², D. G. Mitchell¹, D. C. Hamilton³ & N. Krupp⁴

The concept of an electrical current encircling the Earth at high altitudes was first proposed in 1917 to explain the depression of the horizontal component of the Earth's magnetic field during geomagnetic storms^{1–4}. *In situ* measurements of the extent and composition of this current were made some 50 years later⁵ and an image was obtained in 2001 (ref. 6). Ring currents of a different nature were observed at Jupiter^{7,8} and their presence inferred at Saturn^{9,10}. Here we report images of the ring current at Saturn, together with a day–night pressure asymmetry and tilt of the planet's plasma sheet, based on measurements using the magnetospheric imaging instrument (MIMI) on board Cassini. The ring current can be highly variable with strong longitudinal asymmetries that corotate nearly rigidly with the planet. This contrasts with the Earth's ring current, where there is no rotational modulation and initial asymmetries are organized by local time effects.

The MIMI instrument¹¹ on the Cassini Saturn orbiter spacecraft comprises three sensors that measure particles in specific energy ranges: (1) the ion and neutral camera (INCA) obtains images of ion and neutral species (~ 3 to >200 keV per nucleon); (2) the charge energy mass spectrometer (CHEMS) measures ions and their charge states (~ 3 to 230 keV per charge); and (3) the low-energy magnetospheric measurement system (LEMMS) measures ions (~ 0.02 to ~ 18 MeV) and electrons (~ 0.015 to ~ 1 MeV). Since its orbit insertion at Saturn on 1 July 2004, Cassini has been making nearly continuous measurements of the charged particle environment. The initial set of orbits were near Saturn's equatorial plane and provided *in situ* sampling of both the plasma sheet¹² and the ring current¹³. It was found that the ring current consists of a high (>1) beta (ratio of particle to magnetic pressure) region extending from $\sim 10 < L < 19R_S$ (where one Saturn radius $R_S = 60,268$ km and L is the magnetic shell parameter), with most of the pressure residing in the range $10 < E < \sim 150$ keV and O^+ ions generally contributing $>50\%$ of the total. Lower-energy (<3 keV) plasma was not an important contributor to the pressure^{13,14} and is not included in the present study.

Beginning in autumn 2006, the inclination of Cassini's orbit was raised gradually to high latitudes, providing the opportunity to make off-equatorial measurements *in situ* with the CHEMS and LEMMS sensors and to obtain images of the ion distribution around the equator using the energetic neutral atoms (ENA) technique by looking down (or up) with the INCA sensor. Briefly, the ENA technique relies on charge exchange between trapped ions and a residual neutral gas that results in fast atoms escaping the system and being sensed as if they were photons. One such image is shown in Fig. 1. The ring current maximum intensity is generally outside the orbit of Rhea; observable intensities may extend beyond the orbit of Titan. Overall, the image in Fig. 1 illustrates that although this interval was chosen specifically as an example with minimal local time/longitudinal structure, the ring current, unsurprisingly, is not the

uniform, symmetric construct postulated in early modelling of Saturn's magnetic field^{9,15}.

Figure 2 shows *in situ* measurements of ion pressure and time-intensity profiles from the CHEMS sensor for days 26–44 of 2007. The pressure profile (Fig. 2a) displays a strong asymmetry in local time, with the night side plasma sheet being much narrower in latitudinal extent ($\sim 30^\circ$ versus $\sim 95^\circ$ on the day side) and less intense by a factor of ~ 10 . Both are centred about Saturn's equatorial plane at a distance of $\sim 20 R_S$ as seen from the coordinates (Fig. 2b–d). The particle intensity spectrogram (Fig. 2e) from CHEMS shows that the energy spectrum is somewhat softer on the day side, and it extends to the upper energy limit (230 keV per charge) of the sensor. Detailed examination of other MIMI data (not shown here) shows that Cassini remained within the magnetosphere at all times. The drop-off in particle pressure early on day 38 is most probably caused by crossing from the plasma sheet into the lobe, perhaps past the last closed field line at $\sim 44^\circ$ latitude at local time $\sim 16:15$. Note that the equivalent crossing on the night side occurred at $\sim 17^\circ$ latitude, somewhat closer to the planet ($\sim 24 R_S$ versus $\sim 26 R_S$).

To investigate this clear asymmetry further, we have performed an analysis of all Cassini orbits from 1 July 2004 (Saturn orbit insertion)

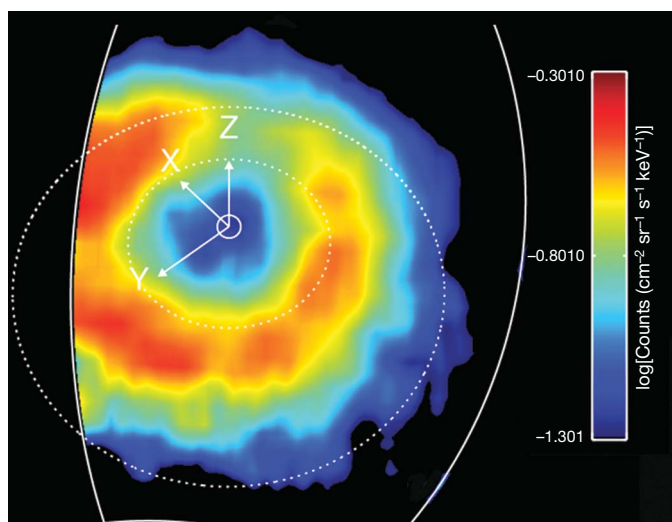


Figure 1 | ENA image of the ring current as viewed from above the northern hemisphere. This image, in the range 20–50 keV, was obtained on 19 March 2007, with MIMI/INCA, at a latitude of $\sim 54.5^\circ$ and radial distance $\sim 24.5R_S$. Saturn is at the centre, and the dotted circles represent the orbits of Rhea ($8.74R_S$) and Titan ($20.2R_S$). The Z axis points parallel to Saturn's spin axis, the X axis points roughly sunward in the Sun–spin-axis plane, and the Y axis completes the system, pointing roughly towards dusk. The INCA field of view is marked by the white line and accounts for the cut-off of the image on the left. The image is a co-spatial average of several frames over the period 16:32–19:44 UTC (Universal time).

¹The Johns Hopkins University Applied Physics Laboratory, Laurel, Maryland 20723, USA. ²Office of Space Research and Technology, Academy of Athens, Soranou Efessiou 4, 11527 Athens, Greece. ³Department of Physics, University of Maryland, College Park, Maryland 20742, USA. ⁴Max-Planck-Institut für Sonnensystemforschung, Max-Planck-Strasse 2, 37191 Katlenburg-Lindau, Germany.

to June 2007. In Fig. 3 the results are plotted in the ρ - Z plane and separated into the day side and night side parts. Figure 3a includes all measured off-equatorial values but excludes the dawn-dusk portion to obtain a clear separation of day-night effects. Although the orbital coverage in Z is not uniform, the higher pressures on the day side appear to extend to much higher latitudes than the night side, certainly at $<20R_S$. This is clearly evident in Fig. 3b, where pressures $<5 \times 10^{-11}$ dynes cm^{-2} have been omitted. Not only is the day-night asymmetry striking, but also the shape of the night side plasma sheet beyond $\sim 20R_S$ is outlined and is seen to be tilted northward at an angle of $\sim 10^\circ$, although the orbital coverage in this region is not extensive. A three-dimensional projection of the pressure distribution at each plane is shown in Supplementary Fig. 1. Examination of each Cassini orbit at all available local times suggests that the day side plasma sheet thins gradually towards the night side, even though the detailed distribution with local time is not fully determined because of incomplete latitudinal/local time coverage.

Our interpretation thus far, based on the pressure distribution, is shown in Fig. 4. This view from above Saturn's equatorial plane illustrates the compressed day side plasma sheet and indicates its expansion to northern and southern latitudes. We expect that the

sheet gradually thins on the dusk side but is drawn tailward at midnight and inflates again at dawn. Whether there is loss of plasma on the night side is not clear, because this sketch represents an average picture of all orbits over a nearly three-year period. We have, however, repeatedly observed acceleration events both in the magnetotail¹⁶ and in parts of the magnetosphere, where the injected plasma cloud clearly corotates with the planet.

One such event is shown in Fig. 5, a sequence of six INCA images covering a Saturn rotation. The top left panel shows a large, factor of ~ 10 , intensity increase between dawn and local midnight that moves

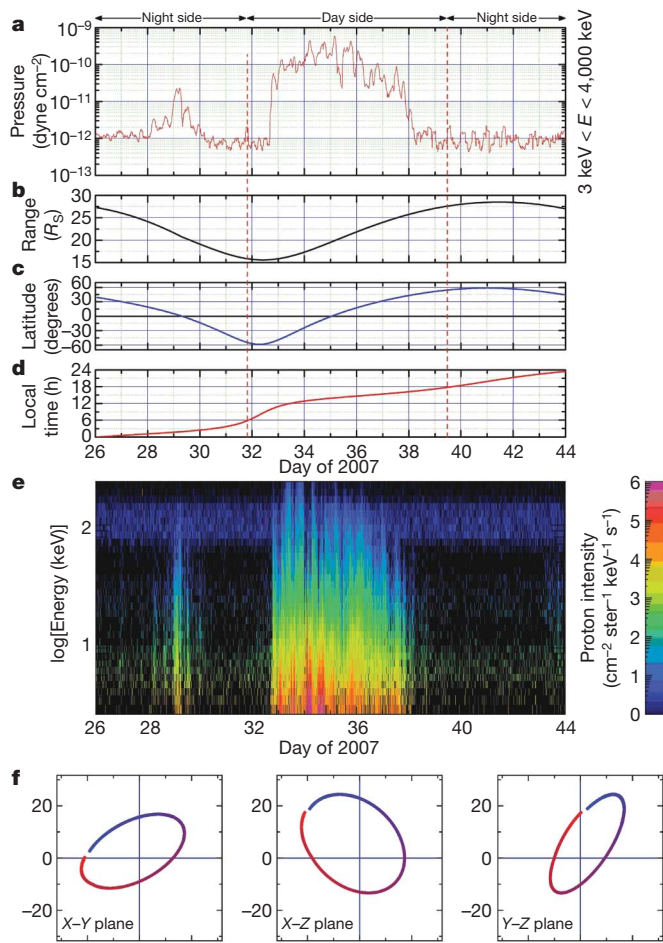


Figure 2 | Typical Cassini pass through the day-night plasma sheet in early 2007. **a**, Ion pressure profile over the indicated time interval. **b–d**, Radial distance, latitude, and local time coordinates of the Cassini spacecraft. **e**, Differential intensity-time spectrogram of protons from the CHEMS sensor over the energy interval $3 < E < 230$ keV per charge; the horizontal dark blue band near the top is background interference and is not relevant. **f**, Projection of the Cassini orbit in the X - Y , X - Z and Y - Z planes in Saturn-centred coordinates; the red and blue colours correspond to inbound and outbound parts of the orbit, respectively.

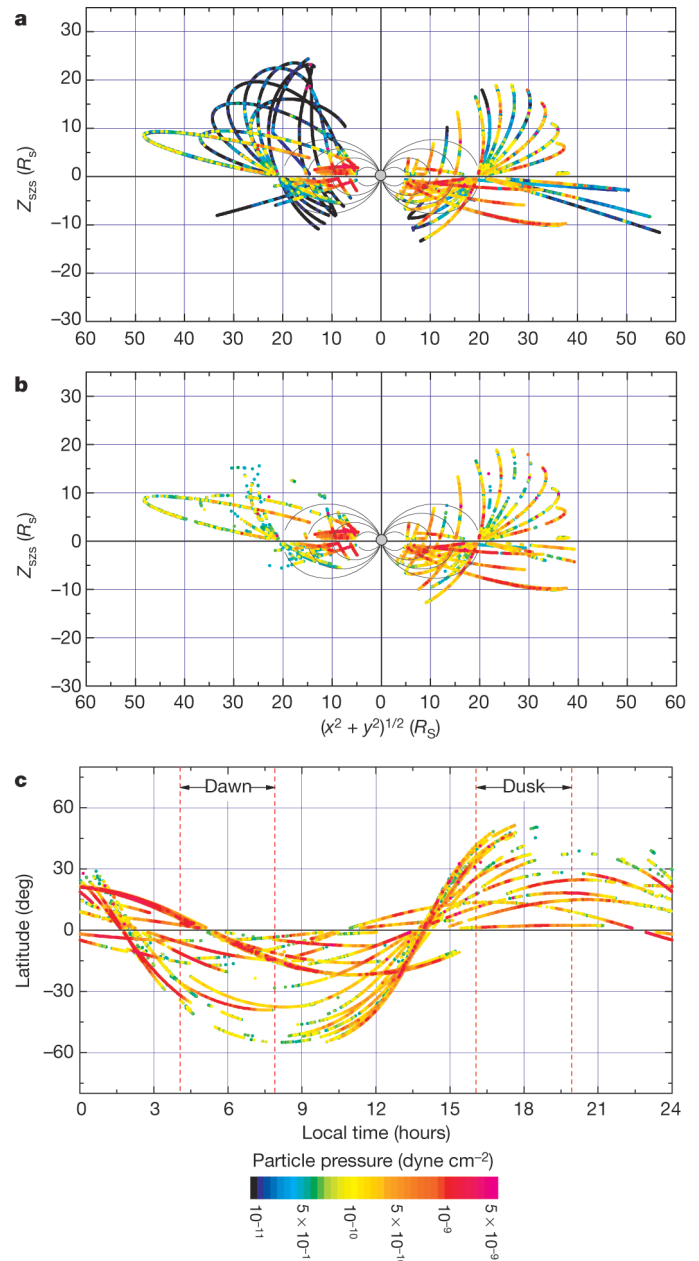


Figure 3 | Observed particle pressure profile (colour scale) for all non-equatorial Cassini orbits. The pressure profile (~ 3 to $4,000$ keV) was computed over the period from July 2004 to June 2007 and is projected onto the $\rho(X^2 + Y^2)^{1/2}$ - Z plane, where X and Y are positions on those axes. **a**, Pressure profile on the day side (08:00–16:00 h, right) and night side (20:00–04:00 h, left) over the full dynamic range measured by the CHEMS and LEMMS sensors (5×10^{-13} to 5×10^{-9} dynes cm^{-2}), clearly illustrating the orbital coverage. **b**, The same data as in **a** but for a threshold $> 5 \times 10^{-11}$ dynes cm^{-2} ; the day-night asymmetry at $R > 20R_S$ is striking. **c**, Pressure coverage in local time and along the Z axis for all thresholded data, but also including the dawn-dusk coverage not shown in **a** or **b**.

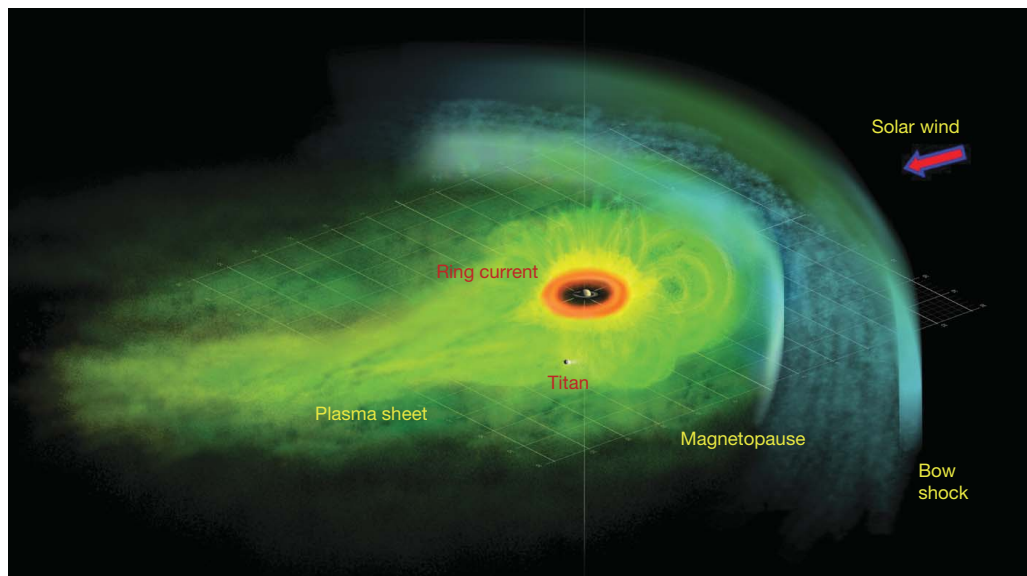


Figure 4 | An artist's concept of Saturn's plasma sheet and embedded ring current, consistent with the data shown in Fig. 3.

Saturn is at the centre, with the red 'doughnut' representing the distribution of dense neutral gas (H , O , O_2 and OH) outside the rings. Beyond this region, energetic ions populate the plasma sheet to the day side magnetopause, filling the faintly sketched magnetic flux tubes to higher latitudes and contributing to the ring current. The plasma sheet thins gradually towards the night side. The view is from above Saturn's equatorial plane, which is represented by grid lines. Titan's location is shown for scale. The location of the bow shock is marked, as is the flow of the deflected solar wind in the magnetosheath.

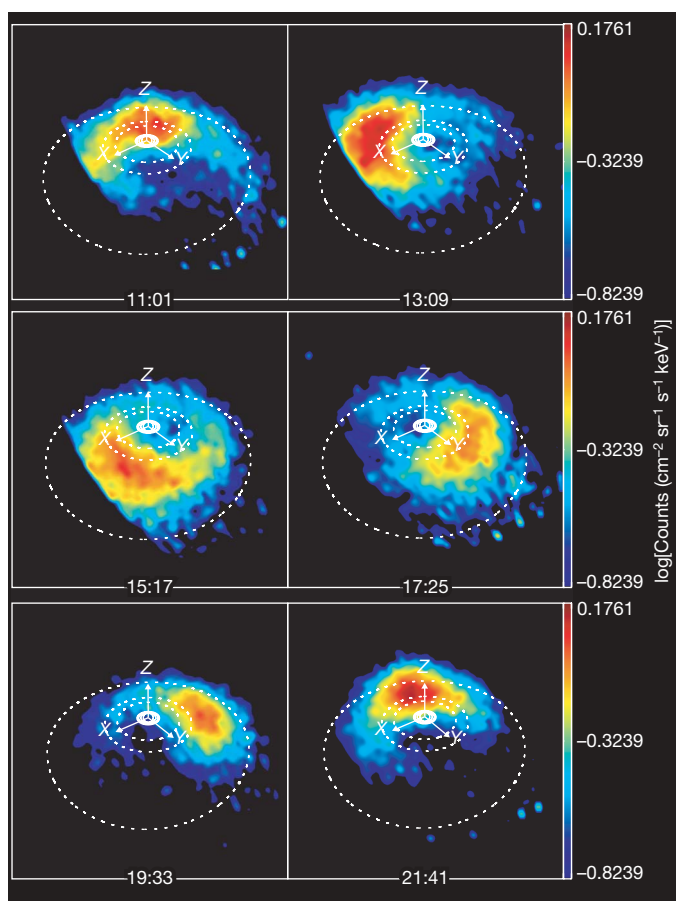


Figure 5 | Sequence of six ENA images in neutral hydrogen taken by INCA. This sequence of ENA images in the range 20–50 keV was obtained on 24 February 2007, and covered a full Saturn rotation. Cassini was located at $\sim 32^\circ$ latitude and $26R_S$ from Saturn at local time $\sim 15:12$. Saturn is at the centre, the X axis is pointing approximately in the solar direction, Y is pointing towards dusk, and Z is pointing along Saturn's spin vector. Dotted lines show the orbits of Dione ($6.26R_S$), Rhea ($8.74R_S$), and Titan ($20.2R_S$) in proper perspective. Sharp edges on the left of the first three frames are attributable to the limit of INCA's field of view. The images are spaced at roughly 2-h intervals. See the Supplementary Video.

anticlockwise through dawn, then day side, then local evening (middle right panel), then local midnight, and then returns to its original location some 11 h later (bottom right panel). Such sequences are seen quite often and are captured in full resolution as movie clips (Supplementary Video). It is clear that in this case, the increase is very nearly fixed in longitude, not local time, and the corresponding ring current is asymmetric and variable. The contribution of such events to the average plasma sheet and ring current sketched in Fig. 4 has not been assessed and is the subject of future study.

The results presented above, using both *in situ* and imaging measurements within Saturn's magnetosphere, demonstrate that the energetic particle pressure contribution to the ring current is far more complex than the ring current initially modelled⁹ as a symmetric region extending from $\sim 9R_S$ to $\sim 15R_S$ in the equatorial plane with a thickness of $\pm 2.5R_S$. Although this early model has been useful until now, the Cassini/MIMI results show that it is a dynamic current system embedded in Saturn's plasma sheet from $\sim 9R_S$ to $\sim 20R_S$, with a vertical extent as high as $\pm 45^\circ$ on the day side. The night side hot-plasma region (ring current/plasma sheet) is tilted above Saturn's equatorial plane with a vertical dimension of $\pm 5R_S$ close in ($< 15R_S$) but extending mostly above that plane to distances of $\sim 50R_S$ and vertically to $\sim 10R_S$. This asymmetry in local time is somewhat consistent with expectations of magnetohydrodynamic simulations¹⁷, and the northward deflection is expected from the tilt of the spin-aligned dipole with respect to the incoming solar wind. The 'hinge' point is predicted to be at $\sim 20R_S$, not inconsistent with the present observations. The day side inflation of the plasma sheet, however, is much greater than that modelled so far¹⁷.

The apparent corotation with the planet of episodically injected plasma, as documented in Fig. 5, represents a conceptual conundrum, in that such plasma blobs are apparently associated with a particular Saturn longitude and are not organized by local time. How the steady-state plasma population can display such obvious day–night asymmetry while the injected particles corotate is a mystery that will require analyses of many more such events.

Received 9 August; accepted 18 October 2007.

- Schmidt, A. Erdmagnetismus. In *Enzyklopädie der Mathematischen Wissenschaften, Band VI* (Teubner, Leipzig, 1917).
- Chapman, S. An outline of the theory of magnetic storms. *Proc. R. Soc. Lond. A* **95**, 61–83 (1918).
- Chapman, S. & Ferraro, V. C. A. A new theory of magnetic storms, Part I. The initial phase. *Terr. Magn. Atmos. Elect.* **36**, 171–186 (1931).
- Chapman, S. & Ferraro, V. C. A. A new theory of magnetic storms. *Terr. Magn. Atmos. Elect.* **38**, 79–96 (1933).

5. Krimigis, S. M. *et al.* Magnetic storm of September 4, 1984: A synthesis of ring current spectra and energy densities measured with AMPTE/CCE. *Geophys. Res. Lett.* **12**, 329–332 (1995).
6. Mitchell, D. G. *et al.* Imaging two geomagnetic storms in energetic neutral atoms. *Geophys. Res. Lett.* **28**, 1151–1155 (2001).
7. Krimigis, S. M. *et al.* Characteristics of hot plasma in the Jovian magnetosphere: Results from the Voyager spacecraft. *J. Geophys. Res.* **86**, 8227–8257 (1981).
8. Mauk, B. M. *et al.* Energetic ion characteristics and neutral gas interactions in Jupiter's magnetosphere. *J. Geophys. Res.* **109**, A09512, doi:10.1029/2003JA010270 (2004).
9. Connerney, J. E. P., Acuña, M. & Ness, N. F. Saturn's ring current and inner magnetosphere. *Nature* **292**, 724–726 (1981).
10. Krimigis, S. M. *et al.* General characteristics of hot plasma and energetic particles in the Saturnian magnetosphere: Results from the Voyager spacecraft. *J. Geophys. Res.* **88**, 8871–8892 (1983).
11. Krimigis, S. M. *et al.* Magnetospheric imaging instrument (MIMI) on the Cassini mission to Saturn/Titan. *Space Sci. Rev.* **114**, 233–329 (2004).
12. Krupp, N. *et al.* The Saturnian plasma sheet as revealed by energetic particle measurements. *Geophys. Res. Lett.* **32**, L20503, doi:10.1029/2005GL022829 (2005).
13. Sergis, N. *et al.* Ring current at Saturn: Energetic particle pressure in Saturn's equatorial magnetosphere measured with Cassini/MIMI. *Geophys. Res. Lett.* **34**, L09102, doi:10.1029/2006GL029223 (2007).
14. Sittler, E. C. Jr *et al.* Cassini observations of Saturn's inner plasmasphere: Saturn orbit insertion results. *Planet. Space Sci.* **54**, 1197–1210 (2006).
15. Mauk, B. H., Krimigis, S. M. & Lepping, R. P. Particle and field stress balance within a planetary magnetosphere. *J. Geophys. Res.* **90**, 8253–8264 (1985).
16. Mitchell, D. G. *et al.* Energetic ion acceleration in Saturn's magnetotail: Substorms at Saturn? *Geophys. Res. Lett.* **32**, L20501, doi:10.1029/2005GL022647 (2005).
17. Hansen, K. C. *et al.* Global MHD simulations of Saturn's magnetosphere at the time of Cassini approach. *Geophys. Res. Lett.* **32**, L20506, doi:10.1029/2005GL022835 (2005).

Supplementary Information is linked to the online version of the paper at www.nature.com/nature.

Acknowledgements We thank M. Kusterer (The Johns Hopkins University Applied Physics Laboratory) for assistance with the data reduction. We are grateful to colleagues on the MIMI team who provided comments that have improved the presentation. Work at The Johns Hopkins University Applied Physics Laboratory was supported by NASA and by subcontracts at the University of Maryland and the Office of Space Research and Technology of the Academy of Athens. The German contribution of MIMI/LEMMS was financed in part by the Bundesministerium für Bildung und Forschung (BMBF) through the Deutsches Zentrum für Luft- und Raumfahrt e.V. (DLR) and by the Max-Planck-Gesellschaft.

Author Contributions S.M.K. is the MIMI Principal Investigator and contributed most of the text; N.S. analysed the *in situ* pressure data; D.G.M. is the INCA lead investigator and analysed the ENA images; D.C.H. is the lead investigator of CHEMS, while N.K. oversees the LEMMS data analyses.

Author Information Reprints and permissions information is available at www.nature.com/reprints. Correspondence and requests for materials should be addressed to S.M.K. (tom.krimigis@jhuapl.edu).